Determination of optimal exposure time for imaging of blood flow changes with laser speckle contrast imaging

Shuai Yuan, Anna Devor, David A. Boas, and Andrew K. Dunn

Laser speckle contrast imaging is becoming an established method for full-field imaging of cerebral blood flow dynamics in animal models. The sensitivity and noise in the measurement of blood flow changes depend on the camera exposure time. The relation among sensitivity, noise, and camera exposure time was investigated experimentally by imaging the speckle contrast changes in the brain after electrical forepaw stimulation in rats. The sensitivity to relative changes in speckle contrast was found to increase at longer exposure times and to reach a plateau for exposure times greater than approximately 2 ms. However, the speckle contrast noise also increases with exposure time and thus the contrast-to-noise ratio was found to peak at an exposure time of approximately 5 ms. Our results suggests that ~5 ms is an optimal exposure time for imaging of stimulus-induced changes in cerebral blood flow in rodents.

OCIS codes: 120.6150, 170.3880, 170.1650.

1. Introduction

Monitoring of cerebral blood flow (CBF) is important for studying both normal and pathophysiologic brain conditions. In particular, the CBF response to a functional stimulus is the basis for many neuroimaging techniques such as functional magnetic resonance imaging. Despite the great interest in monitoring CBF, imaging of CBF changes with high spatial and temporal resolutions has been difficult to achieve. Currently, the two main optical techniques for *in vivo* monitoring of blood flow in animal models are laser Doppler flowmetry (LDF) and laser speckle contrast imaging (LSCI). These techniques have considerable advantages over traditional techniques, such as thermal or radioisotope clearance methods,[1,2] since the optical techniques provide rapid continuous measures of blood flow dynamics.

Although LDF is widely accepted as a standard method for *in vivo* measurement of relative CBF changes, most LDF studies are limited to a single spatial location. In these measurements, a fiber-optic probe is placed on the exposed surface of the cortex, and the CBF dynamics at that location are recorded with high temporal resolution (millisecond). It is possible to obtain spatial information with LDF, although, some form of scanning is typically introduced to achieve this spatial information, which comes at the expense of temporal resolution. For example, Forrester *et al.*[3] reported an acquisition time of more than 4 min to produce a 256×256 point image using scanning laser Doppler. This trade-off between spatial and temporal resolution limits the use of scanning laser Doppler in many studies of functional activation.

LSCI (Refs. 4 and 5) is a technique that overcomes many of the shortcomings of scanning laser Doppler. In particular, since it is a full-field technique that utilizes standard CCD cameras and lasers, there is no trade-off between spatial and temporal resolution. In LSCI, the scattered laser light from the surface of the cortex produces a speckle pattern, which is imaged onto a camera. By analyzing the spatial statistics of the speckle pattern, one determines the speckle contrast, which can be related to a measure of blood flow.[5] LSCI and other similar speckle-imaging techniques have been used to image blood flow in the retina, skin, and other tissues.[6–15] More recently,

S. Yuan, A. Devor, D. A. Boas, and A. K. Dunn (adunn@nmr.mgh.harvard.edu) are with the Martinos Center for Biomedical Imaging, Massachusetts General Hospital, 149 13th St, Charlestown, Massachusetts 02129. S. Yuan is also with the Department of Electrical and Computer Engineering, Tufts University, Medford, Massachusetts 02145.

Received 10 August 2004; revised manuscript received 16 November 2004; accepted 5 December 2004.

0003-6935/05/101823-08$15.00/0

LSCI has been demonstrated to be particularly effective in imaging CBF changes in animal models.[16] Recent studies of CBF have included migraine headache,[17] functional activation of whisker barrel cortex in rats,[18] forepaw activation in rats,[19] mouse physiology,[20] stroke,[21] and cerebral autoregulation.[22]

Because of multiple scattering and the complexity of the underlying physics, it is very difficult to determine absolute blood flow velocity from LSCI measurements. Fortunately, however, measures of relative CBF are extremely useful in studies of functional activation and cerebral pathophysiology. Like LDF, LSCI can measure large changes in CBF, such as those encountered in ischemia and cortical spreading depression, as well as changes of only a few percent such as those found in some functional activation studies. When the changes in speckle contrast are only a few percent, it becomes important to optimize the measurement parameters. The camera exposure time is one such parameter, since the measured speckle contrast changes are a function of the exposure time. Although the relation between exposure time and speckle contrast has been well documented,[5] the effect of camera exposure time on the sensitivity to speckle contrast changes has not been systematically addressed. In this paper the sensitivity of the speckle contrast changes to camera exposure time is analyzed experimentally and theoretically. Measurements of speckle contrast changes in response to functional stimulation in rats at different exposure times indicate that both the sensitivity and the noise of the speckle contrast measurements depend on the exposure time. Therefore an optimal exposure time exists that maximizes the contrast-to-noise ratio (CNR) of the speckle contrast changes.

2. Theory

The speckle contrast, K, is a measure of the local spatial contrast of a speckle pattern and can be used to estimate blood flow velocity. It is defined as the ratio of standard deviation to the mean intensity in a small region of the speckle image,[8]

$$K = \frac{\sigma_s}{\langle I \rangle}, \tag{1}$$

In practice, a 5×5 or 7×7 region of pixels is used to compute K. These values are typically chosen to balance the trade-off between statistical accuracy, which is improved with a larger region, and spatial resolution, which is improved with a smaller region.

To minimize the error of the computed speckle contrast, it is necessary that the average speckle size in the imaging plane closely match the camera pixel size. For image speckle, the speckle size is determined by the aperture size of camera lens and the laser wavelength and is given by

$$d = 2.44\lambda f/_{\#} M, \tag{2}$$

Here λ is the laser wavelength, $f/_{\#}$ is the F-number of camera lens, and M is the magnification of the imaging system.

The spatial variance of the intensity of the time-integrated speckle image, σ^2, is equal to the time average of the autocovariance of the intensity fluctuations, C_t (Ref. 23),

$$\sigma^2(T) = \frac{1}{T}\int_0^T C_t(\tau)\mathrm{d}\tau, \tag{3}$$

where T is the camera exposure time. Therefore the spatial variance, as well as the speckle contrast, is a function of the camera integration time. At very long exposure times the speckle contrast approaches 0, whereas at very short exposure times the speckle contrast should approach 1 since very little blurring of the speckles occurs at short exposure times.

The autocovariance of the speckles depends on the underlying velocity distribution of the scattering particles, and for Brownian motion (Lorentzian power spectrum of the velocity distribution),[23] Eq. (3) can be evaluated analytically and the speckle contrast expressed as[4]

$$K(T) = \frac{\sigma_s}{\langle I \rangle} = \left\{\frac{\tau_c}{2T}\left[1 - \exp\left(\frac{-2T}{\tau_c}\right)\right]\right\}^{1/2}, \tag{4}$$

where τ_c is the autocorrelation decay time of the speckle intensity fluctuations and can be assumed to be inversely proportional to blood velocity ($\tau_c \propto 1/\nu$).[24] Therefore Eq. (4) can be used to relate the measured speckle contrast to the blood flow changes by examining the relative changes in τ_c. The relation of K and T is plotted in Fig. 1(a).

The sensitivity of LSCI to changes in blood flow depends on the exposure time, T. The sensitivity to both absolute flow changes ($\Delta\nu$) and to relative flow changes ($\Delta\nu/\nu$) can be estimated from Eq. (4). We define the absolute sensitivity, S_a, for measurement of absolute flow changes as

$$\begin{aligned} S_a = \left|\frac{\mathrm{d}K}{\mathrm{d}\nu}\right| &\propto -\tau_c r \frac{\mathrm{d}K}{\mathrm{d}\left(\frac{T}{\tau_c}\right)} = -\tau_c r \frac{\mathrm{d}K}{\mathrm{d}r} \\ &= \tau_c \frac{r}{2K}\left[\frac{1}{2r^2} - \frac{(2r+1)}{2r^2}\exp(-2r)\right], \end{aligned} \tag{5}$$

Here we define r as T/τ_c for convenience. S_a indicates the change in speckle contrast value with unit change in mean flow velocity. Figure 1(b) shows a plot of $S_a(T)$ versus r. S_a is a maximum when $T \sim \tau_c$. Usually, in most applications, $T > \tau_c$ in the region where S_a decreases as the exposure time T increases.

In most measurements of CBF changes, the parameter of interest is the relative change in CBF ($\Delta\nu/\nu$). The sensitivity to relative changes in flow can be defined as the ratio of the relative speckle contrast

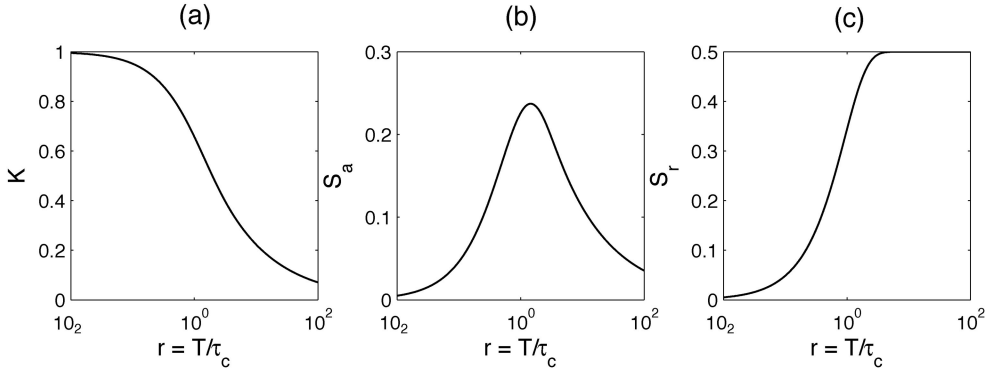

Fig. 1. Theoretical plots of speckle contrast K, absolute sensitivity S_a and relative sensitivity S_r.

change to the relative velocity change:

$$S_r = \left| \frac{\frac{dK}{K}}{\frac{d\nu}{\nu}} \right| = -\frac{\frac{dK}{K}}{\frac{dr}{r}} = -\frac{r}{K}\frac{dK}{dr} = \frac{1}{2K^2}\left[\frac{1}{2r} - \frac{(2r+1)}{2r}\exp(-2r)\right]. \quad (6)$$

The characteristics of S_r are different than that of S_a. Plot of S_r against r is shown in Fig. 1(c). When the exposure time $T < 1.8\tau_c$, S_r increases quickly as the exposure time increases and when $T > 1.8\tau_c$. S_r remains at approximately its maximum level. This maximum value of S_r is 0.5, which means, the relative speckle contrast response is, at most, half of the actual relative flow change.

3. Methods

LSCI was used to image blood flow in the rat somatosensory cortex during electrical forepaw stimulation. By varying the camera exposure time during each stimulation trial, the sensitivity of the stimulus induced changes in speckle contrast as a function of exposure time was determined.

Male Wistar rats ($n = 6$) weighing 250 to 350 g were used for the experiments. Rats were anesthetized with a 50 mg/kg bolus of α-chloralose followed by continuous intravenous infusion at 40 (mg/kg)/h. Body temperature was kept constant at 37 °C with a homeothermic blanket during experiments. Animals were ventilated and breathed room air supplemented with oxygen. A 6 mm × 6 mm portion of the skull overlying the somatosensory cortex was thinned to transparency, and a well was formed around the thinned portion of the skull by use of petroleum jelly and was filled with mineral oil.

The experimental setup is shown in Fig. 2. The diode laser (785 nm, 70 mW) beam was expanded with a collimating lens ($f = 10$ mm) to a size of approximately 20 mm × 10 mm to provide even illumination of the exposed area of cortex. The illuminated area was imaged onto a CCD camera (RoperScientific Coolsnap *fx*) via a camera lens ($f = 60$ mm, $f/_{\#} = 4$–22) with a magnification of 0.22 ~ 0.25. The $f/_{\#}$ of the lens was adjusted to best match the speckle size in imaging plane with the pixel size. The optimal $f/_{\#}$ can be calculated from Eq. (2). For a particular experimental configuration, the optimal $f/_{\#}$ can also be determined by measurement of the speckle contrast as a function of $f/_{\#}$. The optimal $f/_{\#}$ results in the greatest speckle contrast value since on average, each pixel will be sampling one speckle. Figure 3 shows the measured speckle contrast versus $f/_{\#}$ in our optical system. The peak at $f/_{\#} = 13.5$ indicates a good match of speckle size and pixel size. From Eq. (2), the optimal $f/_{\#}$ for our system is approximately 14.4, which is very close to the measured value.

Raw speckle images were converted to speckle contrast images by use of Eq. (1) with 7 × 7 pixels. During the conversion, background noise in the raw speckle image was subtracted prior to speckle contrast calculation.

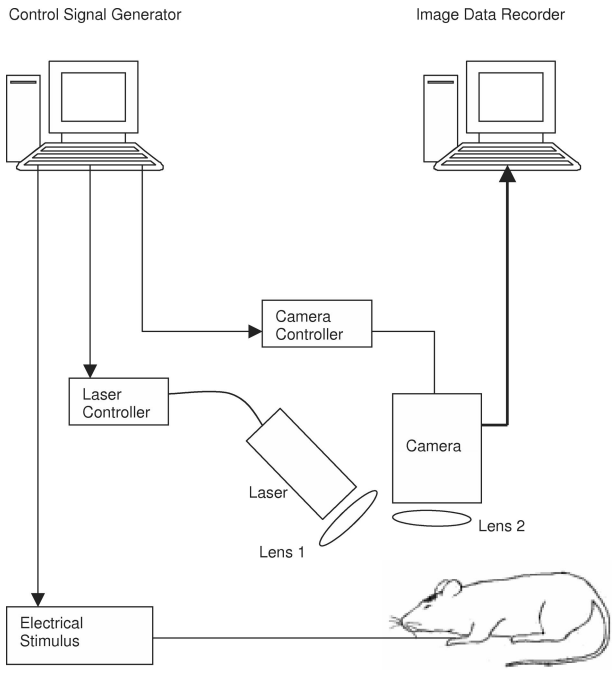

Fig. 2. Experimental setup for laser speckle contrast imaging (LSCI) of CBF during electrical forepaw stimulation.

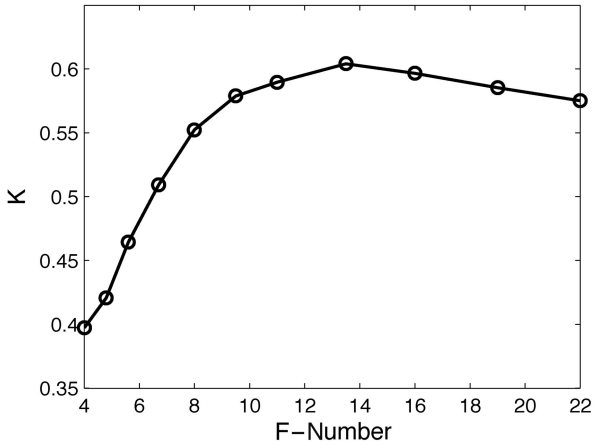

Fig. 3. Measured speckle contrast as a function of $f_{\#}$, where the peak speckle contrast indicates the optimal match between the speckle size and the pixel size.

Forepaw stimulation was delivered through two needles inserted into the contralateral forepaw. Each stimulation trial consisted of 2 s of baseline followed by 4 s of stimulation, which consisted of 300 μs pulses delivered at 3 Hz. The amplitude of each pulse was 1 mA, and stimulation trials were repeated every 30 s.

The effective camera exposure time was varied within each stimulation trial rather than across separate trials to avoid trial-to-trial variations in the CBF response. The camera exposure time was fixed at 20 ms, and we varied the effective exposure time by pulsing the laser diode in synchrony with the camera. Computer-controlled pulses of varying durations and amplitudes were sent to the laser driver to vary the effective exposure time between 0.5 and 20 ms. The amplitude of each laser pulse was set to maintain the same total intensity for each exposure time. Within each stimulation trial, 6 different pulse widths (0.5, 1, 2, 5, 10, 20 ms) were randomly interleaved at 15 Hz.

4. Results

Figure 4 illustrates how the baseline speckle contrast from the exposed cortex varies with different exposure times. The calculated speckle contrast from a 5.6 mm × 6 mm area of cortex is shown for exposure times of 0.5, 5, and 20 ms. As expected, the speckle contrast values for the shorter exposure times are greater than those of longer exposure times. The large blood vessels are clearly seen at all three exposure times. However, the detailed microvascular structures are more apparent at an exposure time of 20 than of 0.5 ms. Since the smaller vessels have a lower flow velocity, and therefore a larger τ_c, than the large vessels, they are observed more clearly at longer exposure times. This clearer observation suggests that the sensitivity of the speckle contrast measurements to small flow differences is greater at longer exposure times.

During each 20-s stimulus trial, all speckle contrast images were divided into six groups according to the effective exposure time (laser pulse widths). For each exposure time the baseline speckle contrast image was defined as the mean speckle contrast at each pixel from $t = 0$ to 2 s. We determined the relative response image by dividing the average speckle contrast over the time $t = 3$–5 s by the baseline speckle contrast for each exposure time. For each animal, 80 stimulation trials were averaged together.

The spatial changes in speckle contrast due to functional activation are illustrated in Fig. 5 for one animal. The exposed area and vasculature are shown in Fig. 5(a) under incoherent green-light illumination. Figure 5(b) shows the relative changes in speckle contrast in the same region with exposure times of T of 0.5, 1, 2, 5, 10, and 20 ms. In Fig. 5(b), the response area is clearly identified in each of the images, where a localized area of decreased speckle contrast is observed, corresponding to an increase in flow velocity. However, the amplitude of the response is quite different for each exposure time. In general, the relative response is stronger and appears more spatially extended with longer exposure times.

To examine the temporal dynamics of the speckle contrast at each exposure time, the mean speckle contrast within a 0.5 mm × 0.5 mm region of interest centered on the peak response was calculated. Since the exposure times were varied randomly within each stimulation trial and also varied from trial to trial,

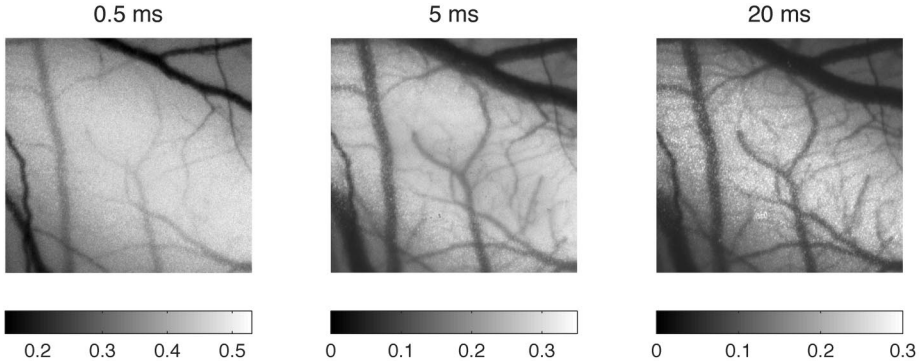

Fig. 4. Speckle contrast images of the somatosensory cortex at exposure times of 0.5, 5, and 20 ms. The imaging area is approximately 5.2 mm × 6.0 mm.

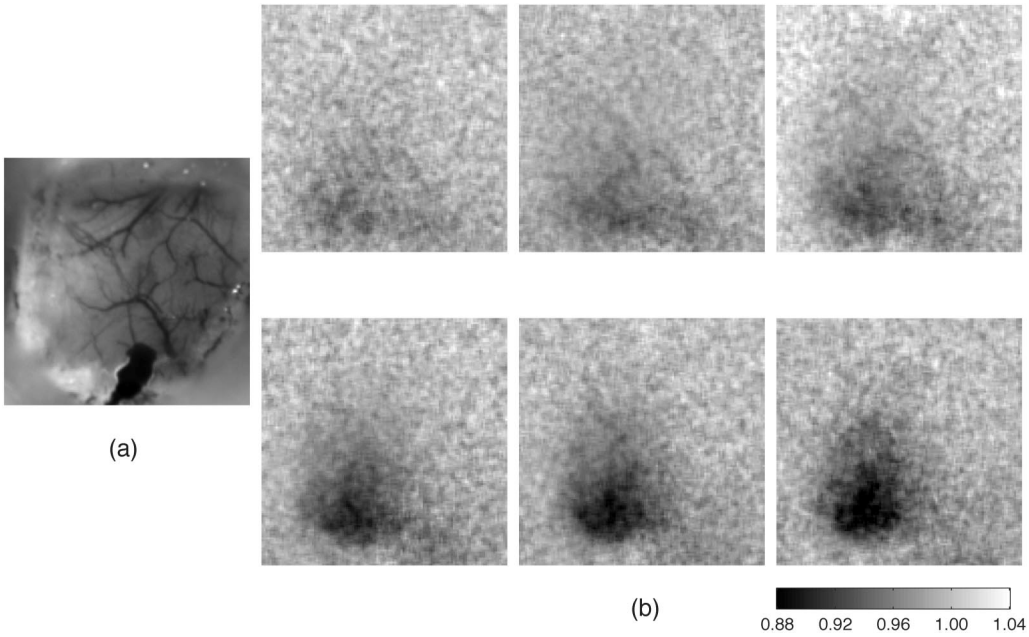

Fig. 5. (a) Image taken with green-light illumination ($\lambda = 560$ nm) illustrating the vasculature; (b) images of the stimulus-induced changes in speckle contrast at different exposure times (0.5 ms to 20 ms). Each image is the ratio of the average speckle contrast over a 2.5-s window after stimulation onset to the average baseline speckle contrast. The imaging area is approximately 5.8 mm $\times$ 5.8 mm.

the timecourse of the speckle contrast signal at each exposure time was interpolated onto a common time scale prior to block averaging of the data. The temporal profile of the relative speckle contrast changes is shown in Fig. 6 for the same animal as in Fig. 5, in which the error bars indicate the standard deviation of the speckle contrast changes across the 80 stimulation trials.

The timecourse of the speckle contrast changes reveals a transient decrease in speckle contrast that recovers to its baseline value within approximately 4 s of the end of the stimulus. The magnitude of the peak change in speckle contrast increases at longer exposure times. This trend was observed in all animals, although the absolute magnitude of the change varied from animal to animal owing to physiologic variation in the response to brain activation.

To quantify the measured sensitivity as a function of the camera exposure time, we calculated the stimulus-induced change in speckle contrast, $\Delta K/K$,

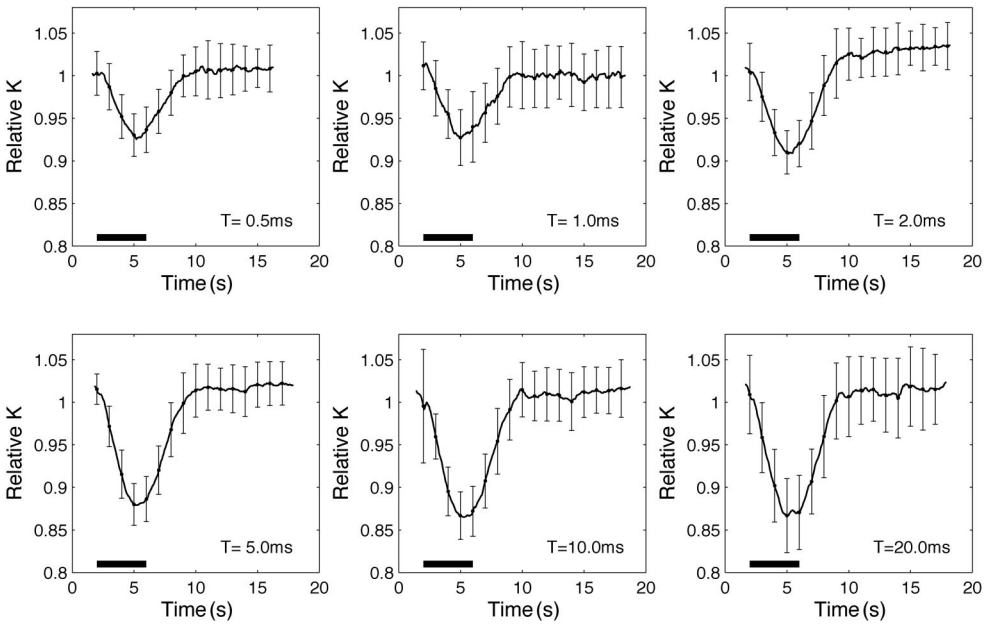

Fig. 6. Timecourse of the speckle contrast changes at each exposure time within a 0.5 mm $\times$ 0.5 mm area centered on the area of activation for one animal. Error bars show the standard deviation over 80 stimulation trials.

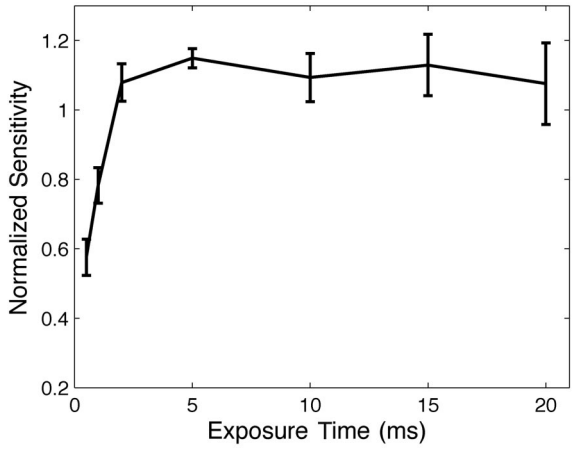

Fig. 7. Experimentally measured sensitivity versus exposure time. The sensitivity for each rat has been normalized to the mean value over all exposure times, and the error bars show the standard error between animals.

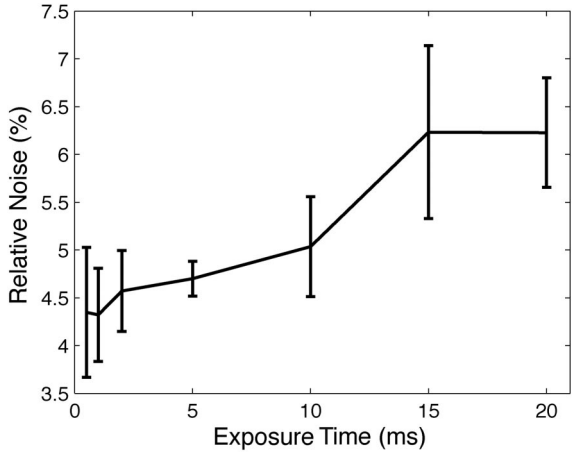

Fig. 8. Relative noise of the speckle contrast signal (σ_K/K) as a function of exposure time. Error bars show the standard error between animals.

for each exposure time, where ΔK is the maximum change in speckle contrast and K is the baseline speckle contrast value. The sensitivity for each animal was then normalized to its mean value over the exposure times from T of 0.5 to 20 ms to account for the animal-to-animal variation in the response amplitudes. Figure 7 shows the measured sensitivity averaged over all animals as a function of camera exposure time and illustrates that the lowest sensitivity is observed at exposure times less than approximately 2 ms. Above this value, however, the sensitivity remains approximately constant as predicted by Eq. (6). The error bars in Fig. 7 show the standard error between animals.

5. Discussion

The shape of the measured relation between the sensitivity to relative speckle contrast changes and the camera exposure time (Fig. 7) is consistent with the theoretical prediction of the relative sensitivity S_r [Fig. 1(c)]. When the exposure time is shorter than some threshold value, the sensitivity decreases sharply, whereas at exposure times longer than the threshold, the sensitivity changes little as the exposure time increases. In Fig. 7, the threshold is approximately 2 ms.

The measured sensitivity curve of Fig. 7 suggests that any exposure time greater than this threshold value will provide optimal sensitivity to blood flow changes. However, the noise in the speckle contrast signal also depends on T and must be considered in addition to the sensitivity function. The measured noise of the baseline speckle contrast signal is shown in Fig. 8 as a function of exposure time. The noise was calculated from the standard deviation of the speckle contrast at each exposure time under baseline conditions (no stimulus), and the relative noise, σ_K/K, is plotted in Fig. 8. The average noise shows an overall increase with increasing exposure time. This trend can also be observed in Fig. 4 where the image noise is greatest at an exposure time of 20 ms.

Several sources of noise contribute to the measured noise in Fig. 8, including physiologic noise, hardware noise, and noise due to statistical uncertainties. Each of these sources exhibit different characteristics with respect to the exposure time. Physiologic noise arises from motion of the tissue such as heartbeat or respiration-induced pulsatile motion of the exposed cortex, as well as baseline fluctuations in the CBF. This motion and blood flow fluctuations introduce additional velocity components to the measured signal and therefore cause speckle contrast fluctuations. The noise introduced by this additional velocity component depends on the camera exposure time. The relative noise due to these physiologic variations, σ_K^{phys}/K, increases at longer exposure times since the physiology noise follows the same relation with exposure time as the sensitivity function, S_r.

Hardware noise comprises several components, but for typical measurements for which the intensity level at the camera is reasonably high, the dominant component of the hardware noise is shot noise. Shot noise introduces an offset in the estimate of the spatial standard deviation and therefore serves as a bias error in the speckle contrast calculation. Since the average integrated light intensity at all of the exposure times was kept reasonably constant, however, the speckle contrast error due to shot noise, σ_K^{shot}, remained constant at all camera exposure times. Therefore the relative noise due to shot noise, σ_K^{shot}/K, varies with exposure time as $1/K(T)$, resulting in a larger contribution at longer exposure times.

Another source of noise is statistical noise, which arises from speckle contrast being derived from statistical quantities. Therefore the accuracy in the estimate of both the mean and the standard deviation of the local intensity depends on the number of pixels used in the calculation, which depends on the size of the $N \times N$ region used in evaluating Eq. (1). A larger number should lead to a more accurate estimate of K

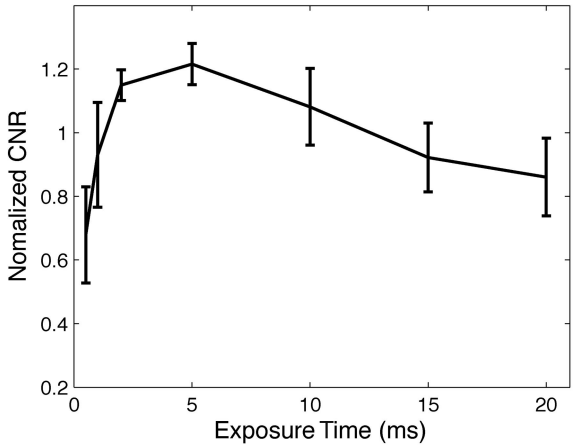

Fig. 9. Normalized CNR as a function of exposure time. Error bars show the standard error between animals.

but also reduces the spatial resolution. One can reduce much of the noise due to statistical uncertainty by additional averaging of speckle contrast images. The error in the estimate of speckle contrast due to this statistical uncertainty is defined by the standard deviation of the estimate of the standard deviation in Eq. (1), which is proportional to the standard deviation itself.[25] Therefore, the statistical noise is proportional to the speckle contrast, and the relative noise, σ_K^{stat}/K, is constant with exposure time.

The total noise of the speckle contrast signal is a combination of physiologic noise, shot noise, and statistical noise. However, the relative contributions of each component are difficult to separate. Given the trend of the speckle contrast noise with exposure time in Fig. 8, however, the physiology and shot noise components are likely to be the dominant sources since the relative noise of each increases with exposure time.

Since both the speckle contrast sensitivity (Fig. 7) and the speckle contrast noise (Fig. 8) increase with exposure time, the optimal exposure time for measurements of functional activation should be determined from the CNR of the stimulus-induced changes in speckle contrast. Figure 9 illustrates a plot of the measured CNR as a function of camera exposure time. The CNR was calculated as $(\Delta K/K)/(\sigma_K/K)$, where $\Delta K/K$ is the stimulus-induced change in speckle contrast and σ_K/K is the relative noise of the baseline speckle contrast signal. The CNR values for each animal were normalized to the mean CNR at all exposure times prior to their being averaged over all animals.

The CNR plot illustrates that the peak CNR is achieved at an exposure time of approximately 5 ms. Although the sensitivity curve (Fig. 7) suggests that the peak sensitivity to speckle contrast changes occurs at any exposure time above a certain threshold, the CNR curve demonstrates that at longer exposure times the increased speckle contrast noise leads to a reduction in CNR. Therefore the optimal exposure time for measurement of stimulus-induced CBF changes in rodents seems to be approximately 5 ms. Despite this particular exposure time perhaps not being optimal for other species and other organs, the underlying principles and methods described here for determination of the optimal exposure time can be used in any setting. The primary difference between speckle contrast imaging of cortical blood flow and blood flow in other organs is differences in baseline blood flow, which result in different baseline levels of speckle contrast, and therefore, τ_c. Therefore it is expected that in applications in which baseline blood flow is greater than that of cortical blood flow, the optimal exposure time will be less than 5 ms, and vice versa.

6. Conclusion

LSCI can be used to image small relative changes in CBF caused by functional brain activation. Both from theoretical deduction and from experiments, we found that the sensitivity of the measured changes in speckle contrast depends on the exposure time. For short exposure times, the sensitivity is low. At the exposure times greater than approximately 2 ms, the sensitivity rises quickly and then remains at approximately the same level for increasing exposure times. Because of the increased noise in the speckle contrast signal at longer exposure times, however, the peak CNR was found at an exposure time of approximately 5 ms. Despite these peak positions being a function of the baseline CBF, the peak is broad and thus the numbers reported here should serve as a guide in choosing an optimal integration time for studies of blood flow changes in rodents, although the theory and methodology are applicable to blood flow imaging in other species.

Support from the Whitaker Foundation and the National Institutes of Health (NS041291, EB000790) is gratefully acknowledged.

References

1. M. Englehart and J. K. Kristensen, "Evaluation of cutaneous blood flow response by Xenon washout and a laser Doppler flowmeter," J. Invest. Dermatol. **80,** 12–15 (1983).
2. A. V. J. Challoner, "Photoelectric plethysmography for estimating cutaneous blood flow," in *Non-invasive physiological measurements*, P. Rolfe, ed. (Academic, London, 1979), Vol. 1, pp. 125–151.
3. K. R. Forrester, C. Stewart, J. Tulip, C. Leonard, and R. C. Bray, "Comparison of laser speckle and laser Doppler perfusion imaging: measurement in human skin and rabbit articular tissue," Med. Biol. Eng. Comput. **40,** 687–697 (2002).
4. A. F. Fercher and J. D. Briers, "Flow visualization by means of single-exposure speckle photography," Opt. Commun. **37,** 326–330 (1981).
5. J. D. Briers, "Laser Doppler, speckle and related techniques for blood perfusion mapping and imaging," Physiol. Meas. **22,** R35–R66 (2001).
6. J. D. Briers and A. F. Fercher, "Retinal blood-flow visualization by means of single-exposure speckle photography," Invest. Ophthalmol. Vis. Sci. **22,** 255–259 (1982).
7. J. D. Briers and S. Webster, "Quasi-real time digital version of single-exposure speckle photography for full-field monitoring of velocity or flow fields," Opt. Commun. **116,** 36–42 (1995).

8. J. D. Briers and S. Webster, "Laser speckle contrast analysis (LASCA): a non-scanning, full-field technique for monitoring capillary blood flow," J. Biomed. Opt. **1,** 174–179 (1996).
9. J. D. Briers, G. Richards, and X. W. He, "Capillary blood flow monitoring using laser speckle contrast analysis (LASCA)," J. Biomed. Opt. **4,** 164–175 (1999).
10. A. K. Dunn, H. Bolay, M. A. Moskowitz, and D. A. Boas, "Dynamic imaging of cerebral blood flow using laser speckle," J. Cereb. Blood Flow Metab. **21,** 195–201 (2001).
11. H. Fujii, "Visualization of retinal blood flow by laser speckle flowgraphy," Med. Biol. Eng. Comput. **32,** 302–304 (1994).
12. N. Konishi and H. Fujii, "Real-time visualization of retinal microcirculation by laser flowgraphy," Opt. Eng. **34,** 753–757 (1995).
13. Y. Aizu, T. Asakura, and A. Kojima, "Compensation of eye movements in retinal speckle flowmetry using flexible correlation analysis based on the specific variance," J. Biomed. Opt. **3,** 227–236 (1998).
14. B. Choi, N. M. Kang, and J. S. Nelson, "Laser speckle imaging for monitoring blood flow dynamics in the *in vivo* rodent dorsal skin fold model," Microvasc. Res. **68,** 143–146 (2004).
15. G. J. Tearney and B. E. Bouma, "Atherosclerotic plaque characterization by spatial and temporal speckle pattern analysis," Opt. Lett. **27,** 533–535 (2002).
16. A. K. Dunn, A. Devor, H. Bolay, M. L. Andermann, M. A. Moskowitz, A. M. Dale, and D. A. Boas, "Simultaneous imaging of total cerebral hemoglobin concentration, oxygenation, and blood flow during functional activation," Opt. Lett. **28,** 28–30 (2003).
17. H. Bolay, U. Reuter, A. K. Dunn, Z. Huang, D. A. Boas, and M. A. Moskowitz, "Intrinsic brain activity triggers trigeminal meningeal afferents in a migraine model," Nat. Med. **8,** 36–42 (2002).
18. A. K. Dunn, A. Devor, H. Bolay, M. L. Andermann, M. A. Moskowitz, A. M. Dale, and D. A. Boas, "Simultaneous imaging of total cerebral hemoglobin concentration, oxygenation, and blood flow during functional activation," Opt. Lett. **28,** 28–30 (2003).
19. T. Durduran, M. G. Burnett, G. Yu, C. Zhou, D. Furuya, A. G. Yodh, J. A. Detre, and J. H. Greenberg, "Spatiotemporal quantification of cerebral blood flow during functional activation in rat somatosensory cortex using laser-speckle flowmetry," J. Cereb. Blood Flow Metab. **24,** 518–525 (2004).
20. C. Ayata, A. K. Dunn, Y. Gursoy-Ozdemir, Z. Huang, D. A. Boas, and M. A. Moskowitz, "Laser speckle flowmetry for the study of cerebrovascular physiology in normal and ischemic mouse cortex," J. Cereb. Blood Flow Metab. **24,** 744–755 (2004).
21. D. N. Atochin, J. C. Murciano, Y. Gursoy-Ozdemir, T. Krasik, F. Noda, C. Ayata, A. K. Dunn, M. A. Moskowitz, P. L. Huang, and V. R. Muzykantov, "Mouse model of microembolic stroke and reperfusion," Stroke **35,** 2177–2182 (2004).
22. S. C. Jones, K. A. Easley, C. R. Radinsky, D. Chyatte, A. J. Furlan, and A. D. Perez-Trepichio, "Nitric oxide synthase inhibition depresses the height of the cerebral blood flow-pressure autoregulation curve during moderate hypotension," J. Cereb. Blood Flow Metab. **23,** 1085–1095 (2003).
23. J. W. Goodman, "Statistical properties of laser speckle patterns," in *Laser Speckle and Related Topics,* 2nd ed. J. C. Dainty, ed. (Springer, Berlin, 1975), pp. 9–75.
24. R. Bonner and R. Nossal, "Model for laser Doppler measurements of blood flow in tissue," Appl. Opt. **20,** 2097–2107 (1981).
25. J. F. Kenney and E. S. Keeping, "The distribution of the standard deviation," in *Mathematics of Statistics, Pt. 2,* 2nd ed. (Van Nostrand, Princeton, N.J., 1951), pp. 170–173.